Analyst

Accepted Manuscript

ROYAL SOCIETY OF CHEMISTRY

www.rsc.org/analyst

A table of contents:

*Graph:

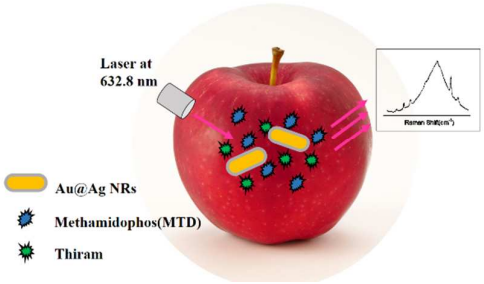

*Text:

A rapid and straightforward method employed to simultaneously detect two pesticides on apple surface.

Cite this: DOI: 10.1039/c0xx00000x

www.rsc.org/xxxxxx

ARTICLE TYPE

Rapid Simultaneous Detection of Multi-pesticide Residues on Apple using SERS Technique

Yizhi Zhang, Zhuyuan Wang*, Lei Wu, Yuwei Pei, Peng Chen, Yiping Cui*

Received (in XXX, XXX) Xth XXXXXXXXX 20XX, Accepted Xth XXXXXXXXX 20XX

DOI: 10.1039/b000000x

A rapid and straightforward method has been employed to simultaneously detect two pesticides (thiram and methamidophos (MTD)) on apple surfaces using surface enhanced Raman scattering (SERS) technique. In the experiment, ethanol was dropped onto the contaminated apple surfaces for the pesticide extraction and then gold@silver core/shell nanorods (Au@Ag NRs) was added to generate the SERS signals of the pesticides. Under a laser excitation at 632.8 nm, prominent SERS peaks of blended contaminants were observed, which were chosen to characterize and quantify their concentration. It was found that SERS intensity of these two peaks changed as a function of the concentration ratio of thiram to MTD. In addition, a better SERS enhancement performance of Au@Ag NRs was demonstrated compared with that of gold nanorods. Our experimental results show that the lowest detectable concentration on apple surfaces is ~4.6×10^{-7} M for thiram and ~4.4×10^{-4} M for MTD, respectively. This study provides a straightforward method for simultaneous detection of multiple pesticides on fruit surfaces, which is important for food safety and human health.

Introduction

Pesticide, which is pervasive in protecting crops and fruits from insects and diseases, plays a crucial role in agricultural production[1–3]. However, with the increasing variety and amount of pesticides employed in agriculture, the threat of pesticide residue to human health is on the rise. Especially some no-standard usage of pesticide, such as overusing, misusing or mixing multiple pesticides, adds the latent hazard to not only human health but also environment and ecology[2,4]. Consequently, the problems of pesticide residues are drawing extensive public attention and worth further investigation.

Up to now, a variety of laboratorial analytical methods have been successfully employed to pesticide detection, including gas chromatography mass spectroscopy (GC-MS), liquid chromatography mass spectroscopy (LC-MS) and high performance liquid chromatography (HPLC) *etc.*.[5–7] In spite of their salient advantages on the quantitative detection, these methods still have limitations such as several-hours-consuming procedure, complicated sample pretreatment or requirement of well-trained laboratory personnel.[8–10] Thus, it is still a challenge to develop a much simpler, faster and more effective method to quantify multiple pesticides simultaneously.

Among the reported detection methods, surface enhance Raman scattering (SERS) is a simple, rapid, nondestructive and accurate technique combining nanotechnology and Raman spectroscopy.[11–13] It can partly remedy the disadvantages mentioned above and has good application prospects in the field of pesticide residue detection.[14–16] Due to the high sensitivity and the 'fingerprint like' signal information provided by SERS [17], much interest has been given to utilize this technique to detect trace amounts of pesticide (*e.g.* organophosphate pesticide, dithiocarbamate fungicide, *etc.*) and the detection sensitivity is continuously improving through ameliorating substrates and optimizing methods.[18–24] Moreover, as the acquisition of SERS spectrum is a rapid and nondestructive procedure, the SERS technique has been expected as one of the best candidates for on-site pesticide detection in real scenario application (*e.g.* fruits, vegetables, meats *etc.*).[9,25–27] However, detecting only one pesticide in food matrices at a time could not meet the real demand in industry due to the combined use of multiple pesticides. Hence, there is an urgent need for on-site multi-pesticide detection techniques. The SERS technique is well-suited for the simultaneous multiplex detection due to the narrow Raman bands with minimal overlapping[28]. The characteristic peaks of various pesticides can be used to easily distinguish each analyte in the mixture, making it possible to detect multi-pesticides through one SERS measurement[29]. This advantage of SERS technique can greatly shorten the detection time and improve the efficiency.

In this study, we aim at exploring the feasibility to simultaneously detect multiple pesticides on apple surfaces using SERS technique. Two pesticides, thiram and methamidophos (MTD), were artificially added onto the apple surfaces and detected simultaneously, as illustrated in Scheme 1. Gold@silver core/shell nanorods (Au@Ag NRs) were used as the SERS substrate due to its good SERS performance. Moreover, to demonstrate the high sensitivity of Au@Ag NRs as SERS substrates, the detection using gold nanorods (GNRs) were also performed for a compared study. To the best of our knowledge, this is the first time that thiram and MTD were quantified

simultaneously on apple surfaces.

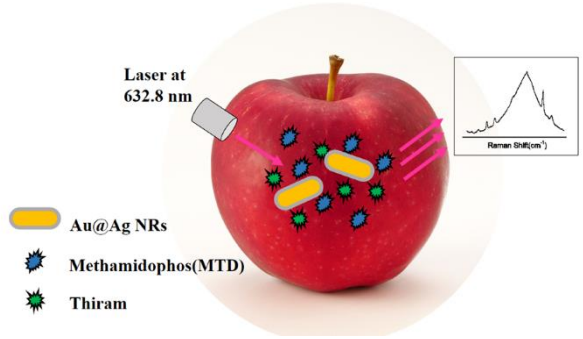

Scheme 1. A schematic illustration of the simultaneous detection of thiram and methamidophos (MTD) on apple surface based on SERS technique.

Experimental Section

Materials

Pesticides thiram powder was purchased from Aladdin Reagent Co., Ltd. (Shanghai, China). Methamidophos (MTD), Hydrogen tetrachloroaurate(III) trihydrate ($HAuCl_4 \cdot H_2O$) and 4-Mercaptobenzoic acid (4MBA) were purchased from Sigma Aldrich. Hexadecyltrimethylammonium bromide (CTAB), sodium borohydride ($NaBH_4$), L-Ascorbic acid (AA) were purchased from Sinopharm Chemical Reagent Co., Ltd. Silver nitrate ($AgNO_3$) was purchased from Shanghai Shenbo Chemical Co., Ltd. Sodium hydroxide (NaOH) was purchased from Guangdong Xilong Chemical Co., Ltd. All reagents are of analytical purity grade. Apples were purchased from a local fruit market. All the reagents were used as received. Deionized water (Millipore Milli-Q grade) with a resistivity of 18.2 MΩ/cm was used in all the experiments.

Preparation of GNRs and Au@Ag NRs

Gold nanorods (GNRs) was synthesized according to the seed-mediated growth method[30]. The obtained GNRs were centrifuged twice at 10000 rpm for 30 min. The synthesis of Au@Ag NRs consulted a method published previously.[31] In a typical experiment, 72.8 mg of CTAB, 4 mL of deionized water, 130 μL of 0.1 M AA, 700 μL of 3 mM $AgNO_3$ and 240 μL of 0.1 M NaOH solution were successively added into 2 mL of the as-prepared GNRs solution under a vigorous stirring to synthesize Au@Ag NRs. The color of the solution changed in two minutes from purple to red, which manifested the constant silver coating.

Preparation of Pesticide Sample

In order to obtain a calibration curve and investigate the limit of detection (LOD), pesticide solutions with sequent concentrations were prepared. Thiram powder was dissolved in ethanol to form a standard stock solution with a concentration of 1 mM. Then the stock solution was diluted with deionized water to prepare pesticides with different concentrations of 0.33, 0.11, 3.7×10^{-2}, 1.2×10^{-2}, 4.0×10^{-3}, 1.3×10^{-3}, 4.6×10^{-4} and 1.5×10^{-4} mM, respectively, in which the latter concentration is one third of the former. 1 mg/mL (~7 mM) MTD water solution was prepared and stocked at low temperature. It was diluted with deionized water into a sequent concentration of 3.5, 1.8, 0.88, 0.44, 0.22, 0.11, 5.5×10^{-2}, 2.7×10^{-2}, 1.4×10^{-2} and 6.8×10^{-3} mM, respectively, in which the latter concentration is one second of the former.

The mixtures of pesticides with various concentration ratios were prepared by mixing 10 μL of MTD and 10 μL of as-prepared thiram with different concentrations together, which formed blended pesticide solutions with a concentration ratio of thiram to MTD being 6.5×10^{-4} : 7, 2.0×10^{-3} : 3.5, 6.0×10^{-3} : 1.8, 1.8×10^{-2} : 0.88.

Preparation of Apple Sample

Carefully cleaned apples were peeled by a fruit knife and the apple peels were cut into nearly uniform squares of ~1 cm^2. These squares were flushed by deionized water, blown dry and placed in a glass dish. Then, 5 μL of the as-prepared pesticide solution with various concentrations was dropped with micropipettes separately onto each apple peel sample and evaporated at room temperature. Referring to the method by Bianhua Liu *et al.*[26], 5 μL of ethanol was dropped onto the sample surface in order to simply extract the pesticide molecules from peels and increase the analyte concentration at the outer surface of peels. After the ethanol completely evaporated at room temperature, 5 μL of concentrated Au@Ag NRs solution was added onto these contaminated peels and remained until totally dry. The blank data on apple surface was obtained from uncontaminated apple samples added with the same amount of ethanol and SERS substrate. The blank data on slide was just signal of the SERS substrate itself, which, in this study, is GNRs and Au@Ag NRs.

Instruments

The formation of GNRs and Au@Ag NRs was monitored by UV-vis spectrophotometer (UV-3600, Shimazu, Japan). Transmission electron microscope (TEM) images were acquired with an FEI Tecnai G2T20 electron microscope operating at 200kV. Centrifugal sample purification was conducted by a high speed centrifuge (2-16PK, Sigma, Germany). SERS measurements were performed with a Raman spectroscopy (T64000, HORIBA JobinYvon, France), using a 632.8 nm laser as an excitation source. Laser power at the sample position was 5 mW. All measures on slides were conducted with a 100×objectives len, 15-s integration time with 2 rounds of accumulation and area scan of 10×10 μm, while the measurements on apple peels were performed with a 50×objectives len, 15-s integration time and 2 accumulations at a single sample position. All SERS spectra in this study were the average result of three measurement results presented with smoothing and baseline adjustment.

Methods of SERS spectra analysis and pretreatment

During the apple skin detection process, it was found that the pristine SERS spectra of pesticide show a strong and wide fluorescence background noise. One of the SERS measurements of 0.3 mM thiram on apple surface is shown in Fig. S1 (red curve). In order to obtain valid characteristic peaks for further analysis, Fast Fourier Transform (FFT) was employed to smooth the spectral curve and remove the background noise by combining with Band-pass Filter. The wide fluorescence noise could be considered as low-frequency signal while the glitch noise on spectral curve could be treated as high-frequency signal. Pristine SERS spectrum was shifted into 'frequency domain' through Fast Fourier Transform and then low and high frequency spectrum was filtered by adjusting the bandwidth of Band-pass Filter. Inversion Fast Fourier

Transform (iFFT) was introduced to reconstruct the filtered spectrum. The built-in function fft(x) and ifft(y) in Matlab was called directly for pretreatment. The treatment result was shown in Fig.S1 (blue curve). Using this method, a smoothing, high signal-noise-ratio SERS spectrum was obtained and the information of characteristic peaks could be easily extracted. In this study, all SERS spectra on apple surface were pretreated through Fast Fourier Transform and Band-pass Filter before analysis.

Results and Discussion

Characterization of GNRs and Au@Ag NRs

It has been reported that silver-coated gold nanoparticles can exhibit a better SERS enhancement factor and particle stability [32,33]. The well performance under the excitation of a 632.8 nm laser has be demonstrated as well.[34,35] Here, we proved the better SERS performance of Au@Ag NRs compared with GNRs in aspect of pesticide detection. As mentioned above, the synthesized GNRs were obtained through the seed-mediated growth method[30]. The TEM image of GNRs is shown in Fig. 1a. The homogeneous and regular core−shell structure of Au@Ag NRs is clearly revealed by the TEM image shown in Fig. 1b.

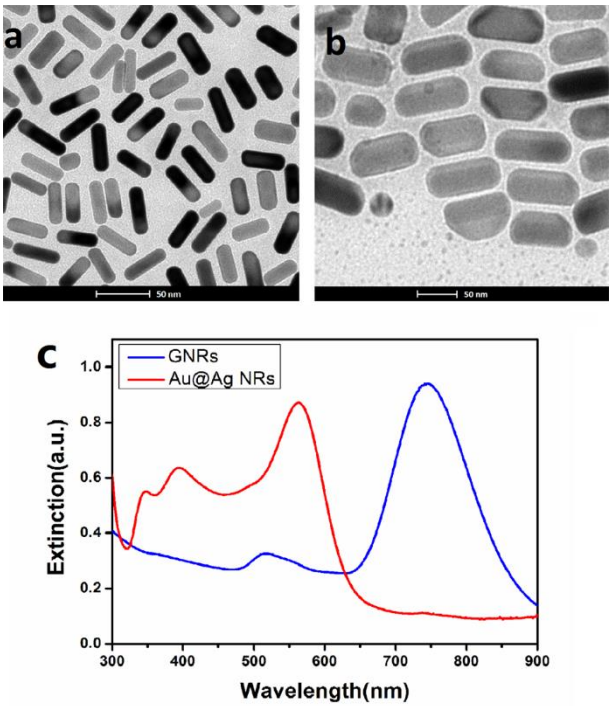

Fig.1. Characterization of GNRs and Au@Ag NRs. TEM images of (a) GNRs and (b) Au@Ag NRs. (c) UV-Vis absorbance spectra of GNRs (blue line) and Au@Ag NRs (red line).

Fig. 1c shows the extinction spectra of Au@Ag NRs (red curve) and GNRs (blue curve). In the case of GNRs, the transverse surface plasmon resonance (SPR) and the longitudinal SPR were observed at 517.5 and 745 nm respectively, indicating the successfully-synthesized rod structure of GNRs[36]. With increasing the thickness of silver shell, average aspect ratio of the core-shell structures has been lowered comparing with the bare gold nanorods, making the longitude SPR at 754 blue-shifts to 563 nm. Meanwhile, a new peak arising from silver appears at 394.5 nm, and a slight bend of the curve at 346.5 nm results from the unsymmetrical structure of the silver shell, which is in agreement with the results by Xiang *et al.*.[31,37]

SERS measurement of single pesticide

To evaluate the enhancement difference of silver coated and uncoated gold nanorods, 20 μL of 0.33 mM thiram solution were exposed to 20 μL of Au@Ag NRs solution and 20 μL of GNRs solution, respectively. The similar experiment was conducted using 20 μL of 1mg/mL (equal to ~7 mM) MTD solution. As shown in Fig. 2, a better enhancement behaviour of Au@Ag NRs is obtained for the detection of both thiram (Fig. 2a) and MTD (Fig. 2b). SERS intensity ratio between Au@Ag NRs and GNRs is ~4-fold for thiram and ~16-fold for MTD. As shown in Fig. 2, main characteristic peaks of thiram are located at 554, 1143, 1375 and 1501cm^{-1}, respectively, which are attributed to υ(S−S), ρ(CH3) or υ(C−N), ρ(CH3) and υ(C−N) [18,26], in consistent with the results in other literatures[22]. Moreover, the enhanced peaks of MTD are at 675, 938, 1296, 1428 cm^{-1}, respectively caused by the C-S vibration symmetry, P-N stretching, N-H bending and –OCH3 bending deformation[38].

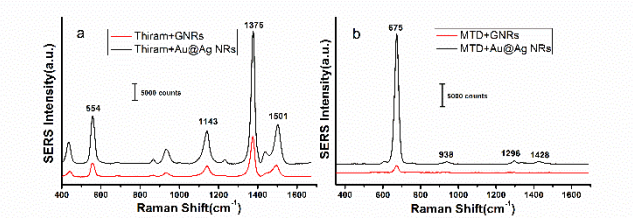

Fig.2. SERS spectra of (a) 0.3 mM thiram solution and (b) 7 mM methamidophos (MTD) in GNRs (red line) and Au@Ag NRs (black line), in which characteristic peaks have been labeled.

Further, solutions of thiram with various concentrations ranging from 0.33 to 1.5×10^{-4} mM were exposed to Au@Ag NRs. As shown in Fig. S2a, a group of SERS spectra exhibit a declining trend as a function of thiram concentration. The strongest peak at 1375 cm^{-1} was chosen as the 'fingerprint' for the quantitative analysis. The dose-response curve is shown in Fig. S2b. The lowest detectable concentration of thiram in Au@Ag NRs is ~1.5×10^{-7}M.

Moreover, the similar experiment and comparison was conducted for MTD. As for MTD, Au@Ag NRs also show an increased enhancement compared with GNRs. Fig. S3a shows the decline trend of SERS spectra as the concentrations of MTD decreased from 0.11 to 6.8×10^{-3} mM. The calibration curve according to the intensity of 675 cm^{-1} peak within the whole concentration range was displayed in Fig. S3b. The detection limit of MTD in Au@Ag NRs is ~6.8×10^{-6}M. As a control, GNRs were employed as the SERS substrate to detect thiram and MTD. The results are shown in Fig. S4 and Fig. S5. It can be found that both SERS intensity and the detection limit of GNRs are less than that of Au@Ag NRs. Specifically, the detection limit of thiram is 4.6 $\times10^{-7}$ while that for MTD is 8.8×10^{-4} M, which is much higher than those by using Au@Ag NRs. Thus, it is clearly demonstrated that silver coated gold nanorods have advantages over the uncoated one in quantifying these two analytes.

Single pesticide residue detection on apple peels

Further, efforts have been made to realize the pesticide detection

on apple surface. We respectively casted the same amount (5 μL) of Au@Ag NRs and GNRs solution on the apple surface to probe the pesticide molecules. Au@Ag NRs-based SERS spectra of thiram with various concentrations are shown in Fig.3a. GNRs-based results are shown in Fig. S6 in supporting information. All these spectra were the average results of three measurements after removing the background using Fast Fourier Transform as mentioned in Experimental Section. Fast Fourier Transform is a better tool to remove the low-frequency fluorescence noise.

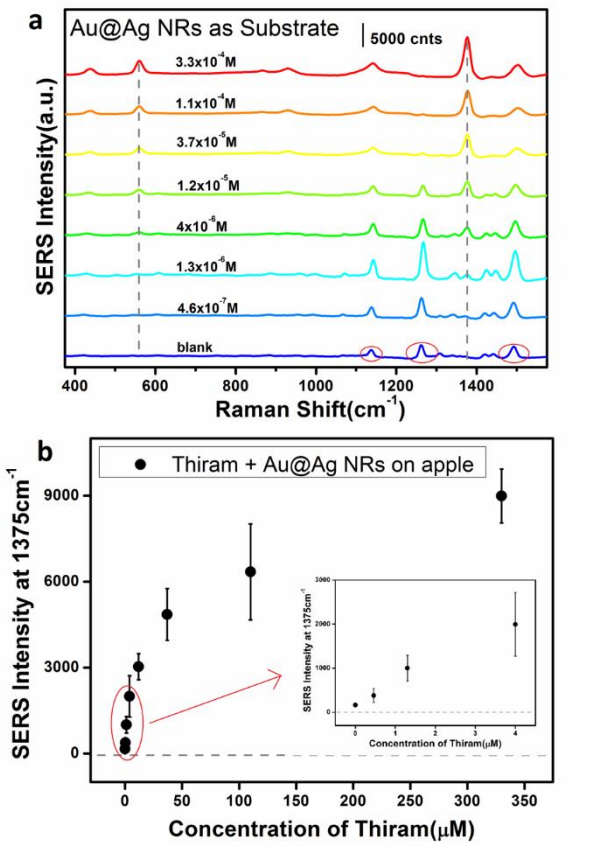

Fig.3. (a) Concentration-dependent SERS spectra and (b) dose-response curve (at 1375cm^{-1}) of thiram on apple peels enhanced by Au@Ag NRs. Inset is the partial enlargement of data points from 4×10^{-6}M to blank on horizontal axis. (The LOD of thiram on apple using Au@Ag NRs is ~4.6×10^{-7}M)

Owing to the ethanol-extraction method[26] mentioned in experiment section, pesticide molecules were well detached from the apple surface, and the spectrum noise of apple peels was lowered. Nanorods solution was dropped on the pesticide molecules and evaporated. These nanorods remained on the outer surface and were close to or adsorbed the pesticide micro-molecules. Under the excitation of incident laser, localized electromagnetic fields or chemical interaction might be formed between closely adjacent or attached target molecules and metallic nanorods[15,24,39] and then SERS signals were obtained. Spectra shown in Fig. 3 clearly reveal that the spectra declined with the decrease of thiram concentration.

In the experiment, it is found that the fluorescent background on apple surface is a high and wide band in the range from approximately 800 to 1400 cm^{-1} (one spectral example shown in Fig. S1). Because of high enhancement quality of Au@Ag NRs and high SERS signal intensity of thiram, the pristine SERS spectra before FFT pretreatment are barely interfered by the noise on apple. While GNRs-amplified signals were not the same (shown in Fig. S6). The weaker peaks were drowned out under the wide noise of apple peels and only strong characteristic peaks of high concentrated pesticide (at 554cm^{-1} and 1375cm^{-1}) can be observed.

Interestingly, some aberrant strong peaks at 1265 and 1495cm^{-1} in low concentration appeared (Fig. 3a), which did not show a sign of concentration-dependence. It is presumed that they might be attributed to some substance on the apple surface or the interaction between apple surface and nanoparticles. Because these peaks could be observed sometimes when no pesticides were added on apple peels (highlighted by red circles shown in Fig. 3a). And due to the uneven surface of apple, the distribution of pesticide molecules and nanorods are inhomogeneous and extremely complicated. Chosen the peak at 1375 cm^{-1} as the fingerprint assessment standard, the calibration curve is displayed in Fig. 3b, revealing that the detection limit of thiram on apple using Au@Ag NRs is ~4.6×10^{-7} M while that using GNRs is ~1.2×10^{-5} M (Fig.S6). That is to say, the consequence on apple also proves the better SERS sensitivity of Au@Ag NRs.

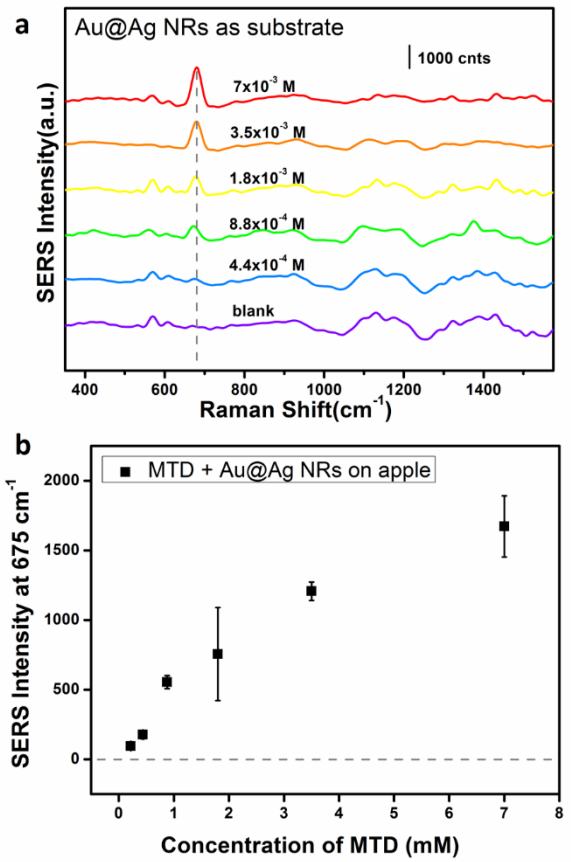

Fig.4. (a) Concentration-dependent SERS spectra and (b) dose-response curve (at 675 cm^{-1}) of methamidophos (MTD) on apple peels using Au@Ag NRs as substrate. (The LOD of MTD on apple using Au@Ag NRs is ~ 4.4×10^{-4}M.)

In terms of MTD detection, we used Au@Ag NRs as the SERS substrate to detect MTD with various concentrations on apple surface by characterizing SERS peaks intensity at 675 cm^{-1}.

Similarly, concentration-dependent SERS spectra and corresponding dose-dependent curve using Au@Ag NRs are revealed in Fig. 4. The lowest detectable concentration on apple surface could reach ~4.4×10^{-4} M. While an attempt has been made to detect concentrated MTD using GNRs, but no signal was observed. The reason might be the weak connection between MTD and GNRs and the relatively weak enhancement performance of GNRs comparing with silver-coated GNRs. Therefore, Au@Ag NRs, due to the better SERS activity for both thiram and MTD detection on real sample, were selected as the substrate for simultaneous multi-pesticide detection.

/mM	Thiram	MTD
A	6.5×10^{-4}	7
B	2.0×10^{-3}	3.5
C	6.0×10^{-3}	1.8
D	1.8×10^{-2}	0.88

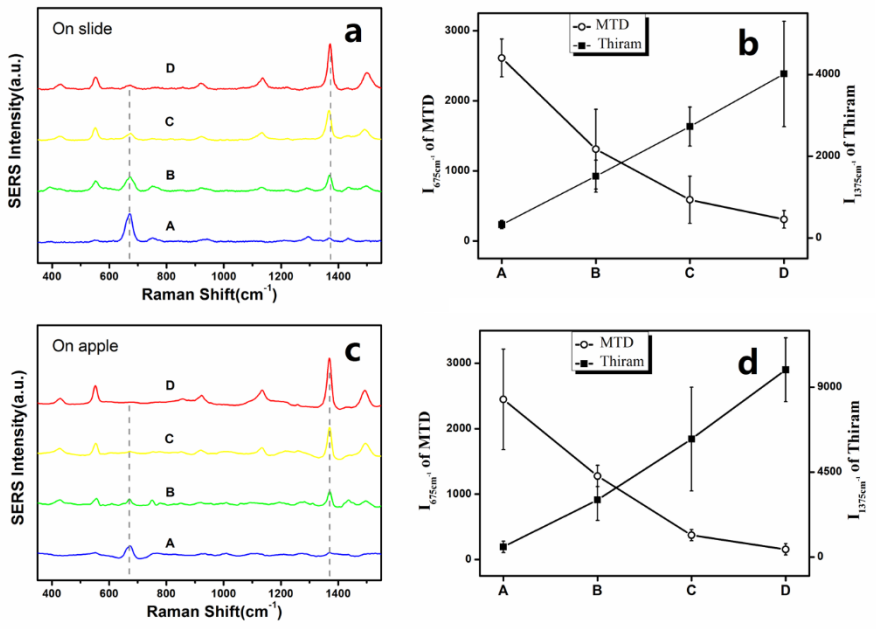

Fig.5. Table: Concentrations of thiram and methamidophos (MTD) in the four groups of mixtures. (a) and (c) are the SERS spectra for the simultaneous detection of thiram and MTD on slide(a) and on apple peels(c) with different concentration ratios. (b) and (d) are the characteristic peak intensity variation curves (1375cm^{-1} for thiram and 675cm^{-1} for MTD) as a function of the mixture concentration ratios on slide(b) and on apple peels(d). The exact concentrations of each group in the mixture were presented in the table.

Simultaneous detection of multi-pesticide on apple peels

In practical applications, for the sake of protection from diseases and insects, multi-pesticides are always blended to spray on crops and fruits, and cause the multi-pesticide residues at the same time. In order to provide an example for the quantitative detection on apple, we mixed these two pesticides with varied ratios and quantify the SERS signal of mixture by using Au@Ag NRs. By comparing the corresponding 'fingerprint' peak intensity, the information of mixture could be obtained.

As shown in Fig. 5(Table), pesticide thiram and MTD were mixed in the concentration ratios of 6.5×10^{-4} : 7, 2.0×10^{-3} : 3.5, 6.0×10^{-3} : 1.8, 1.8×10^{-2} : 0.88. From Fig.5a, it can be distinctly observed that peaks intensity at 1375 and 675 cm^{-1} varied as a function of the mixture proportion (thiram to MTD). As mentioned in experiment section, these blended pesticide solutions were prepared by adding the same volume of thiram and MTD with various concentrations. The volumes of the mixtures are consistent but the amount of pesticides varied. The peaks intensity at 1375 and 675 cm^{-1} were enhanced enormously and did not overlap, which could provide the identification and quantification basis for each pesticide in the mixture. Taking these two peaks as the assessment standard, SERS intensity variation of thiram and MTD with different mixing proportion is manifested in Fig.5b. From the result, we found that peak intensity at 1375 cm^{-1} ($I_{1375cm^{-1}}$) gradually became stronger with the increase of thiram concentration while that at 675 cm^{-1} ($I_{675cm^{-1}}$) became weaker with the decrease of MTD concentration.

Afterwards, the mixture of thiram and MTD with different proportion was pipetted onto apple peels and SERS spectra using Au@Ag NRs as the substrate were shown in Fig. 5c. The corresponding peak intensity variation was shown in Fig. 5d. The consequence on apple is highly consistent with the previous detection result in analytical circumstance, which indicates that quantitative simultaneous detection of thiram and MTD on apple surface has been achieved using Au@Ag NRs as SERS substrate. Through one SERS measurement, the information of thiram and MTD could be simultaneously distinguished using this demonstrated method.

Conclusions

In summary, the SERS-based method to simultaneously quantify thiram and methamidophos (MTD) on apple surface was achieved based on their distinct SERS signals with few sample pretreatment. The total analytical time from pesticide extraction to SERS measurement only cost 30 min. In addition, Au@Ag NRs were demonstrated to show a better SERS activity and higher sensitivity compared with GNRs in this application. This research provides a quantitative analytical reference for the simultaneous detection of thiram and MTD. This straightforward method probably can be used for other pesticides to ensure food safety.

Acknowledgement

This research was supported by National Science Foundation of China (Grant Nos. 60708024, 60877024, 61177033 and 61275182), the Specialized Research Fund for the Doctoral Program of Higher Education (SRFDP) (Nos. 20070286058, 20090092110015), the Scientific Research Foundation of Graduate School of Southeast University (No.YBJJ1328), the Scientific Innovation Research Foundation of College Graduate in Jiangsu Province (No.CXZZ13_0088), the Science Foundation for the Excellent Youth Scholars of Southeast University and the Fundamental Research Funds for the Central University.

Notes and references

Advanced Photonics Centre, School of Electronic Science and Engineering, Southeast University, 2 Sipailou, Nanjing, Jiangsu, China. Email: cyp@seu.edu.cn; wangzy@seu.edu.cn; Fax: +86 25 83790201; Tel: +86 25 83792470 ext. 8208

† Electronic Supplementary Information (ESI) available: [details of any supplementary information available should be included here]. See DOI: 10.1039/b000000x/

1. E. K. Fodjo, S. Riaz, D.-W. Li, L.-L. Qu, N. P. Marius, T. Albert, and Y.-T. Long, *Anal. Methods*, 2012, **4**, 3785.
2. Y. Li, Y. Sun, Y. Peng, S. Dhakal, K. Chao, and Q. Liu, 2012, **8369**, 83690I–83690I–6.
3. P. Raghu, T. Madhusudana Reddy, B. E. Kumara Swamy, B. N. Chandrashekar, K. Reddaiah, and M. Sreedhar, *J. Electroanal. Chem.*, 2012, **665**, 76–82.
4. L.-K. Chai and F. Elie, *Food Control*, 2013, **32**, 322–326.
5. I. Lavagnini, A. Urbani, and F. Magno, *Talanta*, 2011, **83**, 1754–62.
6. E. D. Tsochatzis, U. Menkissoglu-Spiroudi, D. G. Karpouzas, and R. Tzimou-Tsitouridou, *Anal. Bioanal. Chem.*, 2010, **397**, 2181–90.
7. J. Manes, M. Fernandez, and Y. Pico, *J. Chromatogr. A*, 2000, **871**, 43–56.
8. C. Shende, A. Gift, F. Inscore, P. Maksymiuk, and S. Farquharson, in *Proceedings of SPIE*, eds. B. S. Bennedsen, Y.-R. Chen, G. E. Meyer, A. G. Senecal, and S.-I. Tu, 2004, vol. 5271, pp. 28–34.
9. L. He, T. Chen, and T. P. Labuza, *Food Chem.*, 2014, **148**, 42–6.
10. S. Pang, T. P. Labuza, and L. He, *Analyst*, 2014, **139**, 1895–901.
11. J. Kneipp, H. Kneipp, and K. Kneipp, *Chem. Soc. Rev.*, 2008, **37**, 1052–60.
12. K. Hering, D. Cialla, K. Ackermann, T. Dörfer, R. Möller, H. Schneidewind, R. Mattheis, W. Fritzsche, P. Rösch, and J. Popp, *Anal. Bioanal. Chem.*, 2008, **390**, 113–24.
13. M. Baibarac, I. Baltog, L. Mihut, a Matea, and S. Lefrant, *J. Opt.*, 2014, **16**, 035003.
14. P. H. B. Aoki, L. N. Furini, P. Alessio, A. E. Aliaga, and C. J. L. Constantino, *Rev. Anal. Chem.*, 2013, **32**, 55–76.
15. J. Vongsvivut, E. G. Robertson, and D. McNaughton, *J. Raman Spectrosc.*, 2010, **41**, 1137–1148.
16. Q.-Q. Li, Y.-P. Du, Y. Xu, X. Wang, S.-Q. Ma, J.-P. Geng, P. Cao, and T. Sui, *Chinese Chem. Lett.*, 2013, **24**, 332–334.
17. L. Guerrini, S. Sanchez-Cortes, V. L. Cruz, S. Martinez, S. Ristori, and A. Feis, *J. Raman Spectrosc.*, 2011, **42**, 980–985.
18. X. Zheng, Y. Chen, Y. Chen, N. Bi, H. Qi, M. Qin, D. Song, H. Zhang, and Y. Tian, *J. Raman Spectrosc.*, 2012, **43**, 1374–1380.
19. X. T. Wang, W. S. Shi, G. W. She, L. X. Mu, and S. T. Lee, *Appl. Phys. Lett.*, 2010, **96**, 053104.
20. L. Wu, Z. Wang, and B. Shen, *Nanoscale*, 2013, **5**, 5274–8.
21. J. F. Li, Y. F. Huang, Y. Ding, Z. L. Yang, S. B. Li, X. S. Zhou, F. R. Fan, W. Zhang, Z. Y. Zhou, D. Y. Wu, B. Ren, Z. L. Wang, and Z. Q. Tian, *Nature*, 2010, **464**, 392–5.
22. B. Saute, R. Premasiri, L. Ziegler, and R. Narayanan, *Analyst*, 2012, **137**, 5082–7.
23. B. Saute and R. Narayanan, *Analyst*, 2011, **136**, 527–32.
24. J. M. Chem, C. Yuan, R. Liu, S. Wang, G. Han, and M. Han, *J. Mater. Chem.*, 2011, 16264–16270.
25. B. Liu, P. Zhou, X. Liu, X. Sun, H. Li, and M. Lin, *Food Bioprocess Technol.*, 2012, **6**, 710–718.
26. B. Liu, G. Han, Z. Zhang, R. Liu, C. Jiang, S. Wang, and M.-Y. Han, *Anal. Chem.*, 2012, **84**, 255–61.
27. X. Li, S. Zhang, Z. Yu, and T. Yang, *Appl. Spectrosc.*, 2014, **68**, 483–7.
28. J. a Dougan and K. Faulds, *Analyst*, 2012, **137**, 545–54.
29. L. Wu, Z. Wang, S. Zong, H. Chen, C. Wang, S. Xu, and Y. Cui, *Analyst*, 2013, **138**, 3450–6.
30. I. Gorelikov and N. Matsuura, *Nano Lett.*, 2008, **8**, 369–73.
31. L. Wu, Z. Wang, S. Zong, Z. Huang, P. Zhang, and Y. Cui, *Biosens. Bioelectron.*, 2012, **38**, 94–9.
32. D. M. Mott, D. T. N. Anh, P. Singh, C. Shankar, and S. Maenosono, *Adv. Colloid Interface Sci.*, 2012, **185-186**, 14–33.
33. S. Pande, S. K. Ghosh, S. Praharaj, S. Panigrahi, S. Basu, S. Jana, A. Pal, T. Tsukuda, and T. Pal, *J. Phys. Chem. C*, 2007, **111**, 10806–10813.
34. A. P. Gold, G. Silver, C. Shell, B. N. Khlebtsov, V. A. Khanadeev, M. Y. Tsvetkov, V. N. Bagratashvili, and N. G. Khlebtsov, 2013.
35. Z. Zhang, S. Zhang, and M. Lin, *Analyst*, 2014, **139**, 2207–13.
36. wNikhil R. J. C. J. Christopher J. Orendorff, Latha Gearheart and Murphy, *Phys. Chem. Chem. Phys.*, 2005.
37. Y. Xiang, X. Wu, D. Liu, Z. Li, W. Chu, L. Feng, K. Zhang, W. Zhou, and S. Xie, *Langmuir*, 2008, **24**, 3465–70.
38. Y. Xie, G. Mukamurezi, Y. Sun, H. Wang, H. Qian, and W. Yao, *Eur. Food Res. Technol.*, 2012, **234**, 1091–1098.
39. E. C. Le Ru, P. G. Etchegoin, and M. Meyer, *J. Chem. Phys.*, 2006, **125**, 204701.

